M. Massari, M. Zamaro
Application of SDRE Technique to Orbital and Attitude Control of Spacecraft Formation Flying
Acta Astronautica, Vol. 94, N. 1, 2014, p. 409-420
doi:10.1016/j.actaastro.2013.02.001

Application of SDRE Technique to Orbital and Attitude Control of Spacecraft Formation Flying

Mauro Massari*, Mattia Zamaro

Dipartimento di Ingegneria Aerospaziale, Politecnico di Milano, Italy

Abstract

This paper proposes the application of a nonlinear control technique for coupled orbital and attitude relative motion of formation flying. Recently, mission concepts based on formations of spacecraft that require an increased performance level for in-space maneuvers and operations, have been proposed. In order to guarantee the required performance level, those missions will be characterized by very low inter-satellite distance and demanding relative pointing requirements. Therefore, an autonomous control with high accuracy will be required, both for the control of relative distance and relative attitude. The control system proposed in this work is based on the solution of the State-Dependent Riccati Equation (SDRE), which is one of the more promising nonlinear techniques for regulating nonlinear systems in all the major branches of engineering. The coupling of the relative orbital and attitude motion is obtained considering the same set of thrusters for the control of both orbital and attitude relative dynamics. In addition, the SDRE algorithm is implemented with a timing update strategy both for the

*Corresponding Author: Ph. +39 2399 8379, Fax. +39 2399 8334

Email addresses: mauro.massari@polimi.it (Mauro Massari), mattia.zamaro@mail.polimi.it (Mattia Zamaro)

controller and the proposed nonlinear filter. The proposed control system approach has been applied to the design of a nonlinear controller for an up-to-date formation mission, which is ESA Proba-3. Numerical simulations considering a tracking signal for both orbital and attitude relative maneuver during an operative orbit of the mission are presented.
Keywords: Formation Flying, Nonlinear Control, State Dependant Riccati Equation, Attitude Control

---

1. Introduction

Formation flying has become an area of great interest for both NASA and ESA since the launch, in 1999, of the latest satellite of NASA Landsat program, Landsat 7. Mission analysis and requirements for the first formations have been very simple and common, as they were constituted by a minimal set of two satellites. Those satellites were placed in a so-called trailing configuration, where the deputy satellite follows the chief along the same orbit. The reasons for such a simple and basic configuration can be inferred from the fact that those formations were designed to increase the performances of Earth observation missions. As a matter of fact, placing two satellites in proximity on the same orbit, makes possible to cover the same ground target area with multiple angles of view and multiple access times. That could allow the use of recent development in radar-based observation instruments to realize 3D mapping and terrain motion monitoring of Earth surface, just adding a second satellite flying in formation with an existing one. This application can highly reduce the response time of synthetic-aperture-radar (SAR) mission in providing differential-interferometric measures of ground target area.

The relative distance between the two satellites can be used to tune the measurements of the interferometric SAR. As in the example just reported, the application of formation flying was firstly devoted to science purposes, with the aim of realizing a complex observation instrument exploiting the relative motion of multiple components. However, the main objective and purpose of a modern formation is the use of multiple spacecraft flying in close proximity for the fulfillment of a common mission requirement, that can be of any kind.

The design of the orbital control system for the kind of formation presented above had been performed using linear control theory applied to the linearized Hill's equations of relative motion. In that case, good control performances have been obtained using the Linear Quadratic Regulator (LQR) [1][2]. The use of simplified models of the dynamics was imposed by the use of linear control theory. However, that was not a great limitation, as the relative distance (in the order of a few km) was sufficiently small to guarantee that the Hill's linearization is accurate.

Nonlinear models and control strategies started to be investigated only in recent years, by the major work of Alfriend, Schaub and Gim,[3][4][5]. The nonlinear approach is required to better exploit the potentialities of formation flying for the design of new mission concept. First of all, the mission design has become more complicated as in the case of the the ESA Cluster II mission launched in 2000. Four satellites have been put on a high elliptic orbit to realize a tetrahedron Cluster Formation which still provides important results on high Magnetosphere dynamics. Second of all, the mission requirements have started to be more demanding as formations at smaller relative distances are designed. Small relative distances require a high-performance

autonomous control to provide the necessary safety. Coordinated coupled control of both orbital and attitude relative motions[6][7][8] becomes essential for other science applications like the case of inertial cluster observation (natural extension of SAR technique). In addition, tracking of relative maneuvers and non-keplerian formations are now demanded for propellant saving optimization. The most anticipated mission in the science world will be the forerunner in a lot of those aspects: LISA (Laser Interferometric Space Antenna) is an interplanetary formation composed by three satellites that NASA and ESA are designing in order to prove the existence of gravitational waves.

Linear control techniques can not provide the high performances required by those new application of formation flying. The model errors will be instantaneously compensated by control actions, increasing the fuel consumption, or in extreme cases, bringing to conditions in which the mission requirement are not satisfied. Nonlinear control techniques allow overcoming the limitations imposed by the linearization of the dynamics. New nonlinear design techniques have been proposed so far: dynamic inversion, sliding mode[9], recursive backstepping[10] and nonlinear adaptive control[10]. However, nonlinear techniques are very sensitive to the dynamics of the case under study, leading to a more complex overall control design with respect to linear techniques.

During the last decade, the State-Dependent Riccati Equation (SDRE)[11][12] innovative nonlinear methodology burst into the automatic control field. This technique has the great advantage of being a systematic procedure, which consists in parameterizing the system dynamics in a pseudo-linear form, with

State-Dependent Coefficients (SDC). Then, the classical optimal control theory and algorithms can be applied to that SDC parametrization, bringing in that way to a State-Dependent Riccati Equation. Mathematical properties and operational strategies of this methodology have been deeply analyzed during that period[11][13][14]. Thanks to the improvement in computational capability of onboard computers, the SDRE technique has also started to be proposed for application to aerospace problems. Example of such problem are the design of autopilots for missile guidance[15] and the control of spacecraft motion[16]. Following an analogous approach it is also possible to derive a SDRE filtering (SDREF) for sensors measurements[17].

In this paper the use of the SDRE methodology is applied to the design of a completely coupled control system (orbital and attitude relative dynamics) for spacecraft in formation. The orbital and attitude dynamics of a spacecraft are naturally coupled by the environmental actions such as the gravitational forces or the atmospheric perturbations. The coupling between the two dynamics is also naturally provided by the reaction thrusters of the spacecraft control system. Misalignment of thrust direction produces a net torque around the center of mass, while directly influencing the orbital dynamics. The choice of considering the coupling of the two dynamics allows the inclusion of the system requirements deriving from the integrated control system directly in the controller design and optimization.

The proposed approach will be applied to a test case which considers the requirements of an up-to-date formation mission, the ESA Proba-3 mission. This mission is constituted by a pair of spacecraft, the Coronagraph (CS) and the Occulter (OS), flying at small distance on a High Elliptical Orbit (HEO).

The dynamical model of Proba-3 formation is derived using the available data provided on the ESA web-site and in the Phase A Summary Report[18]. That model is used to evaluate the performances of a coupled control system based on the SDRE methodology, for both the controller and the nonlinear filter.

The paper is organized as follows. The model used to describe the formation flying relative dynamics is formulated in the next section, which is followed by an overview of the SDRE methodology. Then, the requirements and details of Proba-3 mission used to carry out the numerical simulation are described together with the details of the implemented timing update strategy for the solution of the SDRE. Finally, the results of the numerical simulations are presented, followed by the conclusions.

2. Formation Flying Relative Dynamics

The relative motion of the members of a formation, called deputies, with respect to a chief satellite, are described using a nonlinear model for both the relative position and attitude dynamics. The chief satellite represents the origin of the reference frame and can be identified with a physical spacecraft or with a non-physical frame of interest for the mission.

2.1. Relative Orbital Dynamics

The relative orbital kinematics can be easily written in the Earth Centered Inertial reference frame (ECI) highlighting the apparent terms as follows:

$$r_d = r_c + \rho \tag{1}$$

$$\ddot{r}_d = \ddot{r}_c + \ddot{\rho} + a_{app} \tag{2}$$

$$a_{app} = [\dot{\omega}_H \wedge \rho + \omega_H \wedge (\omega_H \wedge \rho)] + 2\omega_H \wedge \dot{\rho} \tag{3}$$

where r_d and r_c are the absolute position respectively of the deputy and of the chief, ρ is the relative position of the deputy in the Hill's reference frame, a_{app} is the apparent acceleration of the deputy and ω_H is the angular velocity of the Hill's reference frame with respect to ECI reference frame.

Using the classical two-body perturbed (2B-P) assumption to model the satellite dynamics in the ECI reference frame, it is possible to express the relative orbital dynamics of the deputy in terms of accelerations as:

$$\ddot{\rho} = -a_{app} + \mu\left(-\frac{r_d}{{r_d}^3} + \frac{r_c}{{r_c}^3}\right) + \left(\frac{a_d^d}{m_d} - \frac{a_c^d}{m_c}\right) + \left(\frac{u_d}{m_d} - \frac{u_c}{m_c}\right) \tag{4}$$

where a_c^d and a_d^d are the disturbances on chief and deputy, u_c and u_d are the control actions on chief and deputy, and m_c and m_d are the masses of chief and deputy.

The relative orbital dynamics is mainly influenced by the apparent acceleration a_{app} of the Hill's reference frame and from the differential accelerations due to the gravitational attraction. Moreover, the relative dynamics is directly influenced by actual differential disturbances and by eventual differential control actions. If the chief and deputy are orbiting in proximity, it is possible to made the assumption that the disturbances are similar and erase each other. The modeling of the perturbed chief dynamics is then used to express the Hill's reference frame kinematics required to compute a_{app}:

$$\omega_H = \begin{bmatrix} \frac{1}{v_\theta} a_h^d \\ 0 \\ \frac{v_\theta}{r} \end{bmatrix} \tag{5}$$

$$\dot{\omega}_H = \begin{bmatrix} \frac{1}{r}a_h^d + \frac{1}{{v_\theta}^2}a_\theta^d a_h^d + \frac{1}{v_\theta}\dot{a}_h^d \\ 0 \\ -2\frac{v_r v_\theta}{r^2} + \frac{1}{r}a_\theta^d \end{bmatrix} \tag{6}$$

where v_r and v_θ are the radial and transverse components of the chief velocity in the orbital plane, while a_θ^d and a_h^d are the component of the disturbance accelerations acting on the chief expressed in the Hill's reference plane along the transverse and normal directions.

2.2. Relative Attitude Dynamics

The relative attitude kinematics is expressed through the use of a rotation matrix Γ that describes the relative orientation of the deputy principal axes of inertia with respect to the chief principal axes of inertia. That matrix is used to express the relative angular velocity and acceleration of the deputy with respect to the chief: whereas no apparent terms come out for the angular velocity, an apparent angular acceleration $\dot{\omega}_{app}$ must be considered.

$$A_d = \Gamma A_c \tag{7}$$

$$\omega_r = \omega_d - \Gamma\omega_c \tag{8}$$

$$\dot{\omega}_r = \dot{\omega}_d - \Gamma\dot{\omega}_c + \dot{\omega}_{app} \tag{9}$$

$$\dot{\omega}_{app} = \omega_r \wedge \Gamma\omega_c \tag{10}$$

where ω_c and ω_d are the angular velocity of the chief and deputy expressed in their principal axes of inertia, while ω_r is the relative angular velocity expressed in the deputy principal axes of inertia.

In order to describe the relative attitude of the deputy a parameterization of the rotation matrix Γ is required. In this work the Modified Rodrigues Parameters (MRP), which are an evolution of the quaternions, are

considered[19]. They are a minimal set of three parameters (which does not compromise system controllability) that are described with two different sets which have the same norm but components with opposite sign. That allows not only to overcome singularities of minimal parameterization, but also to intrinsically describe every rotation with the minor angle definition (which is given by the norm-limited MRP set). The MRP are defined by the following relations:

$$\sigma = \frac{\tilde{q}}{1 + q_0} \tag{11}$$

$$\Gamma(\sigma) = I_3 - \alpha_1^A [\sigma\wedge] + \alpha_2^A [\sigma\wedge]^2 \tag{12}$$

$$\begin{cases} \alpha_1^A = 4\frac{1-\sigma^T\sigma}{(1+\sigma^T\sigma)^2} \\ \alpha_2^A = 8\frac{1}{(1+\sigma^T\sigma)^2} \end{cases} \tag{13}$$

where σ are the MRP, $\tilde{q}$ are the quaternions and I_3 is an identity matrix.

The kinematics relationship which bind the MRP to the angular velocity is the following:

$$\dot{\sigma} = \tfrac{1}{4}\Sigma(\sigma)\,\omega \tag{14}$$

$$\Sigma(\sigma) = \left(1 - \sigma^T\sigma\right) I_3 + 2\sigma\sigma^T + 2[\sigma\wedge] \tag{15}$$

The relative attitude dynamics can be obtained substituting kinematics relationships in the Euler absolute equation for the deputy spacecraft:

$$J_d\dot{\omega}_r + \omega_r \wedge J_d\omega_r = -M_g - M_{ci} + M_{app} + M_d + T_d \tag{16}$$

where J_d is the matrix of inertia of the deputy, M_d are disturbance torques and T_d are control torques. The relative attitude dynamics is influenced by gyroscopic torques M_g, chief-inertial torques M_{ci} and apparent torques M_{app}:

$$M_g = M_{gc} + M_{gcoup} \tag{17}$$

$$M_{gc} = \Gamma\omega_c \wedge J_d\Gamma\omega_c$$

$$M_{gcoup} = (\omega_r \wedge J_d\Gamma\omega_c + \Gamma\omega_c \wedge J_d\omega_r)$$

$$M_{ci} = J_d\Gamma\dot{\omega}_c \tag{18}$$

$$M_{app} = J_d\omega_r \wedge \Gamma\omega_c \tag{19}$$

2.3. Coupled Relative Dynamics

The dynamics equations shown above can be used to simulate formation dynamics with proper initial conditions, applied control actions and appropriate disturbance modeling. The modeling of the space environment is extremely important in designing every space mission. The magnitude of force and torque perturbations is highly dependent on the operative orbit and size of the spacecraft. However, the most relevant perturbations are always present for Earth orbiting satellites and can be summarized in: gravitational forces from Earth not homogeneous gravity field; Sun-Moon attraction; gravity gradient torques; torques induced by the interaction with Earth magnetic field; forces and torques deriving from electromagnetic radiation pressure and atmospheric drag. The orbital and attitude dynamics of a spacecraft are naturally coupled by these environmental perturbations.

The non-gravitational perturbations are orientation-dependent forces and torques, which are relevant, if compared to basic gravitational term, only for very low orbit trajectories (drag) and in the case of very big solar panels (solar radiation). Position-dependent torques are instead very relevant for attitude control of Earth satellites: basic Earth gravity gradient torque has indeed been used as a passive stabilizing strategy. Other perturbation torques

are relevant only in specific cases. The only coupling terms of the dynamics considered in the controller design is the gravity gradient torques on deputy, for which the analytic expression is reported here:

$$M_{GG} = 3\frac{\mu}{r_d^5} r_d \wedge J_d r_d \tag{20}$$

The coupling between the two dynamics is also naturally provided by the reaction thrusters of the spacecraft control system. Misalignment of the thrust direction produces a net torque around the center of mass. Therefore, the control actions required to influence the orbital dynamics directly influence also the attitude dynamics.

3. The SDRE Methodology

Consider the general control-affine nonlinear system of first-order differential equations:

$$\dot{x} = f(x) + g(x)\, u \tag{21}$$

where $x(t)$ are the states and $u(t)$ are the control actions. A systematic procedure to derive a controller for the dynamics has been proposed by Cloutier, D'Souza and Mracek[11][12]. In this procedure a point-wise linear-like description of the differential equations is considered. Every nonlinear equation which satisfies the following analytical requirements,

$$x \in \mathbb{R}^n, u \in \mathbb{R}^m \tag{22}$$

$$f(x) \in \mathcal{C}^k, g(x) \in \mathcal{C}^k, k \geq 1 \tag{23}$$

$$\begin{cases} f(0) = 0 \\ g(x) \neq 0, \forall x \end{cases} \tag{24}$$

can be written in a pseudo-linear form where all coefficients are state-dependent (State Dependent Coefficient or SDC parametrization):

$$\dot{x} = A(x)x + B_u(x)u + B_d(x)d \tag{25}$$

where $d(t)$ are the disturbances.

Even in the case that the analytical requirements are not fully satisfied, Cloutier presented a technique to derive a correct SDC form of the system dynamics[13]. In addition, the presence of different pseudo-linear forms for the nonlinear systems, which is often considered an issue of the approach, is turned into an advantage. In fact, it is possible to consider a proper linear combination of the different SDC forms, implicitly adding degrees of freedom (the weighting parameters) to the controller design[20].

3.1. SDRE-based Controller

With the dynamics expressed in SDC form, it is possible to apply the classical optimal control theory. Making the assumption of infinite-horizon (IH) control and following the same approach as in the Linear Quadratic Regulator (LQR). Let define a state-dependent quadratic cost functional $\Im(x, u)$ of the state and control vectors:

$$\Im(x, u) = \frac{1}{2}\int_0^\infty x^T Q(x)x + u^T R(x)u dt \tag{26}$$

where $Q(x)$ and $R(x)$ are weighting matrices respectively on states and controls. Those state-dependent weighting matrices should satisfy the same requirements deriving from the classical linear optimal control theory. In particular, Q and R should be symmetrical, with the first one positive-semidefinite and the second one strictly positive-definite. Moreover, the

controllability of $[A, B_u]$ pair, and the observability of $[A, q]$ pair (where q is a proper factorization of Q) should be guaranteed. The minimization of the cost functional subject to the system dynamics constraint, requires the satisfaction of two necessary conditions. The first one, as in the LQR formulation, allows to derive the control gain matrix, that will be used in the nonlinear optimal control law:

$$K(x) = R^{-1}(x){B_u}^T(x)P(x) \tag{27}$$

$$u(x) = K(x)x \tag{28}$$

The second one is the Hamilton-Jacobi-Bellman equation (HJB), that is used to derive the sensitivity matrix P:

$$\begin{aligned} &\dot{P}x + \left[x^T {A_{/x_i}}^T + u^T {B_{u/x_i}}^T\right]^T Px + \tfrac{1}{2}\left[x^T Q_{/x_i} x + u^T R_{/x_i} u\right] + \\ &+ \left[A^T P + PA - PB_u R^{-1} {B_u}^T P + Q\right] x = 0 \end{aligned} \tag{29}$$

This condition can be divided in two parts: the first one is called necessary condition for optimality, and collects all the derivatives of the state-dependent matrices; the second one represents the State-Dependent Riccati Equation (SDRE):

$$A^T P + PA - PB_u R^{-1} {B_u}^T P + Q = 0 \tag{30}$$

It has been proved that the terms of the first part of the HJB equation tend to zero as the state vector reaches the equilibrium. Therefore, the solution is obtained solving only the SDRE, which gives the point-wise stabilizing control law along the state trajectory[11]. The SDRE technique can be considered as a linear-like parametrization of the Optimal Control for nonlinear systems, where the additional terms are related to the existence of multiple

SDC forms. In these cases, the solution obtained is sub-optimal. The control performances should always be tested with computer simulations, since the original nonlinear system stability, controllability and observability cannot be matched tout-court to the SDC system properties.

3.2. SDREF

The SDC parametrization of the system is also suitable to be observed with the dual SDRE algorithm, that allows the derivation of a Kalman-like nonlinear filter. Consider the dual dynamical system:

$$\dot{\hat{x}} = A(\hat{x})\hat{x} + B_u(\hat{x})u + B_d(\hat{x})d + L(\hat{x})\left[y - C(\hat{x})\hat{x}\right] \tag{31}$$

where y is the measured state:

$$y = C(x)x + D(x)u \tag{32}$$

The estimator control law, expressed by the SDC gain matrix L, is derived via a dual optimization algorithm[17], whose weighting matrices on states and controls can be summarized as:

$$\begin{cases} N(\hat{x}) = B_d(\hat{x})W_{dd}(\hat{x}){B_d}^T(\hat{x}) \\ V(\hat{x}) = D_{yr}(\hat{x})W_{rr}(\hat{x})D^T(\hat{x}) \end{cases} \tag{33}$$

The estimator control law is then:

$$L(\hat{x}) = \Lambda(\hat{x})C^T(\hat{x})V^{-1}(\hat{x}) \tag{34}$$

where the classic assumption of no correlation of the process disturbances with the measurements and relative noises is considered.

The sensitivity matrix Λ is derived from HJB equation, resulting from the point-wise solution of the dual SDRE optimization, approximating the related necessary condition for optimality:

$$\begin{aligned}&\dot{\Lambda}\hat{x} + \left[\hat{x}^T A_{/\hat{x}_i} + y^T C_{/\hat{x}_i}\right]\Lambda\hat{x} + \tfrac{1}{2}\left[\hat{x}^T N_{/\hat{x}_i} o + y^T V_{/\hat{x}_i} y\right] + \\ &+ \left[A\Lambda + \Lambda A^T - \Lambda C^T V^{-1} C\Lambda + N\right]\hat{x} = 0\end{aligned} \tag{35}$$

Again, the first part of the HJB equation tends to zero as the state vector reaches the equilibrium. Therefore, the solution is obtained solving only the dual SDRE:

$$A\Lambda + \Lambda A^T - \Lambda C^T V^{-1} C\Lambda + N = 0 \tag{36}$$

4. SDRE Control System Design for PROBA-3

Proba-3 is ESA's first close formation flying mission. Its technological objective is the demonstration of new in-space technologies, to assure close relative maintenance and operations. The mission is constituted by a pair of spacecraft, the Coronagraph (CS) and the Occulter (OS), flying at small distances in High Elliptic Orbit (HEO). The operative orbit is divided in two phases: across the slow apogee passage, the operative configuration is maintained, while the configuration is untied during the remaining part of the orbit. The operative configuration is obtained letting the OS fly in front of the Sun to cast a shadow across the CS, eclipsing the Sun and allowing the observation of the Corona. The scientific objective of the mission is actually the study of the inner solar corona, so the orbit of the CS is not fixed but it is designed to have its apogee aligned with the daily Sun direction. During the untied configuration phase other manoeuvres and technologies are tested.

Scientific data are downloaded to ground stations during the fast perigee passage.

The proposed control system approach has been applied to the design of the relative orbital and attitude control of the OS. Therefore, the CS dynamics is used as a reference signal (using quaternions as attitude parametrization) for the deputy relative motion and its control system. The chief orbital motion is considered uncontrolled, while the assumption of a chief attitude control system working ideally has been made. Figure 1 shows the architecture of the simulation used to test the designed control system.

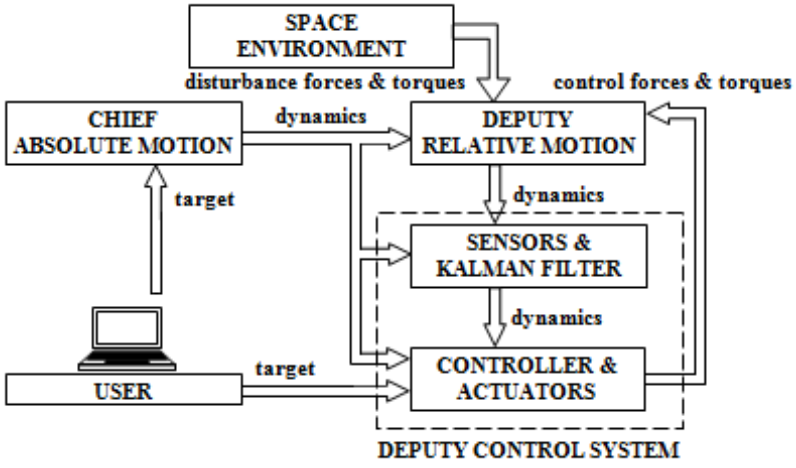

Figure 1: Formation Flying control system block diagram.

The deputy control system makes use of a Kalman-like nonlinear filter designed with the dual SDRE procedure (which is the SDREF) for the reconstruction of the state vector from sensors measurements. That state is compared with a tracking signal to compute the error that the designed SDRE-based controller uses to command the coupled Orbital and Attitude

Control System (OACS) of the deputy (the OS).

4.1. Mission Analysis and Requirements

The control system performances are investigated using an adequate modeling of Proba-3 mission specifications. The Chief HEO is derived from available data presented on the ESA website of the mission, and is characterized by apogee and perigee heights of $60524km \times 800km$. The orbit is assumed to be J_2-free, for propellant saving, and placed in the ecliptic plane. Finally, the remaining argument of perigee is derived orienting the apogee to be Sun-pointing at the current day of orbit simulation. The CS is assumed to have nadir pointing attitude during all the orbit.

The deputy trajectory is divided in two parts. During the central part of the orbit, crossing the apogee, the OS is maintained in operative configuration, which is approximated as it is placed in front of the chief in the radial direction, at a distance of $150m$. During the first and last third of the orbit, crossing the perigee, the formation is relaxed in a trailing configuration, maintaining the same relative distance. Therefore, two specular relative reconfiguration manoeuvres are required to switch between those configurations. Each manoeuvre is obtained imposing a tracking signal that describes a one-quarter circular path, with uniform acceleration motion, along the transversal relative coordinate (the first half with positive acceleration, the second one with negative acceleration). The total time of the manoeuvre (T_m) is fixed in 2 hours. Figure 2 shows the CS absolute orbit in ECI and the OS relative orbit in the chief Hill's reference frame.

In addition, the orbital reconfiguration manoeuvre is accompanied by a relative attitude reconfiguration, assuming that the OS communication

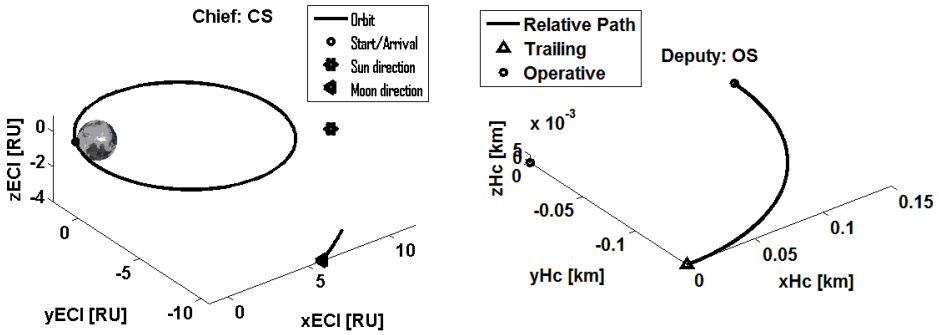

Figure 2: Coronagraph spacecraft absolute orbit and Occulter spacecraft relative orbit.

side is always oriented to point in the direction of the CS. The CS and OS inertial properties are derived considering a parallelepiped architecture with dimensions and mass based on the available mission data.

4.2. SDC Parametrization of formation flying relative dynamics

The control system design is performed considering a state vector which encloses the states of both the orbital and attitude dynamics. In particular the state vector includes the relative position and velocity, the relative attitude described used the MRP and the angular velocity. In the following the chosen SDC form of the relative position and attitude dynamics will be presented.

Considering the relative orbital dynamics, the nonlinearity is present in the differential gravitational action, and the equations are easily taken to the unique pseudo-linear form:

$$-\left(\frac{\mu}{{r_d}^3}r_d - \frac{\mu}{{r_c}^3}r_c\right)_{Hc} = \left(-\frac{\mu}{{r_d}^3}I_3 + \mu\xi_r \begin{bmatrix} 2r_c+\rho_r & \rho_\theta & \rho_h \\ 0 & 0 & 0 \\ 0 & 0 & 0 \end{bmatrix}\right)\rho \tag{37}$$

$$\xi_r = \frac{1}{{r_c}^2{r_d}^3}\frac{(r_c+r_d)^2 - r_c r_d}{(r_c+r_d)} \tag{38}$$

where ρ_r, ρ_θ and ρ_h are the components of the relative position vector in the Hill's reference frame of the chief.

The MRP kinematics relationship does not allow a single SDC parametrization but it is the typical case in which multiple SDC forms must be combined to obtain a suitable SDC formulation. This is done adding parameters to weight the different formulations. In this work two SDC parametrization for the MRP kinematics are used. In the first SDC form considered the state matrix components related to the MRP and angular velocity are present, while in the second one mixed quadratic terms between MRP components are contained. The two SDC form are combined using a single weighting parameter $\alpha_{\omega\sigma}$:

$$\dot{\sigma} = \alpha_{\omega\sigma}\frac{1}{4}\Sigma(\sigma)\omega + (1-\alpha_{\omega\sigma})\left(\frac{1}{4}\Sigma^{\omega}(\sigma,\omega,\alpha_\sigma)\sigma + \frac{1}{4}I_3\omega\right) \tag{39}$$

The integral states of relative position and MRP are adjoined to the state vector in order to allow a proper tracking of the orbital and attitude reference signal. In addition, the system is augmented with a three-components stable state s, whose values are fixed to unity, in order to consider the bias terms in the attitude dynamics. The relative bias eigenvalue is chosen in a way that makes its dynamics consistently slower than the attitude dynamics response

time: the value used is 0.001 rad/s.

$$\dot{s} = -\lambda_s I_3 s \tag{40}$$

The above mentioned bias terms come out in writing the chief states (angular velocity and acceleration) in the deputy principal axes of inertia reference frame. An example of the suggested procedure to treat the bias terms is reported here for a generic vector v (other three additional parameters are present in the resulting matrix Ψ):

$$\Gamma(\sigma)v = Diag\left\{\frac{v_i}{s_i}\right\} s + \left(\alpha_1^A \left[v\wedge\right] + \alpha_2^A \Psi(\sigma, v, \alpha_\sigma)\right)\sigma \tag{41}$$

where $\Gamma(\sigma)$, α_1^A and α_2^A are defined in Eq. (12) and (13).

Besides, considering the coupling effect of the gravity gradient torque on the attitude dynamics, a bias term results from the SDC parametrization of its definition in Eq. (20), and is treated with two matrices M_{54} and M_{56}:

$$\begin{aligned} M_G = {} & 3\tfrac{\mu}{r_d{}^5}\left[\Gamma(\sigma)\Delta(q_c)r_d\wedge\right] J_d\Gamma(\sigma)\Delta(q_c)\rho + \\ & + r_c 3\tfrac{\mu}{r_d{}^5}\left[\Gamma(\sigma)\Delta(q_c)r_d\wedge\right] J_d\Gamma(\sigma)\Delta(q_c)\begin{bmatrix}1\\0\\0\end{bmatrix} \end{aligned} \tag{42}$$

$$\Gamma(\sigma)\Delta(q_c)\begin{bmatrix}1\\0\\0\end{bmatrix} = \left(\Gamma(\sigma)\Delta(q_c)\right)_{1stcol} = M_{54}(q_c,\sigma)\sigma + M_{56}(q_c,\sigma)s \tag{43}$$

where Δ is the rotation matrix describing the orientation of the Hill's reference frame with respect to the chief principal axes of inertia, expressed using the quaternions q_c.

In conclusion, after the definition of a 21-components state vector:

$$x = \begin{bmatrix} \rho_I & \rho & \dot{\rho} & \sigma & \omega & s & \sigma_I \end{bmatrix}^T \tag{44}$$

where ρ_I and σ_I are the integral states, the resulting state matrix and disturbance matrix, which introduces perturbing accelerations in the dynamics, can be outlined as:

$$A(x) = \begin{bmatrix} 0_3 & I_3 & 0_3 & 0_3 & 0_3 & 0_3 & 0_3 \\ 0_3 & 0_3 & I_3 & 0_3 & 0_3 & 0_3 & 0_3 \\ 0_3 & A_{32}(x) & A_{33} & 0_3 & 0_3 & 0_3 & 0_3 \\ 0_3 & 0_3 & 0_3 & A_{44}(x) & A_{45}(x) & 0_3 & 0_3 \\ 0_3 & A_{52}(x) & 0_3 & A_{54}(x) & A_{55}(x) & A_{56}(x) & 0_3 \\ 0_3 & 0_3 & 0_3 & 0_3 & 0_3 & A_{66} & 0_3 \\ 0_3 & 0_3 & 0_3 & I_3 & 0_3 & 0_3 & 0_3 \end{bmatrix} \tag{45}$$

$$B_d = \begin{bmatrix} 0_3 & 0_3 & I_3 & 0_3 & 0_3 & 0_3 & 0_3 \\ 0_3 & 0_3 & 0_3 & 0_3 & I_3 & 0_3 & 0_3 \end{bmatrix}^T \tag{46}$$

4.3. OACS Implementation

The relative orbital and attitude dynamics are controlled using the same set of thrusters, coupling in this way the two dynamics. This coupling effect is not necessary desirable from the point of view of the control system design and performances. However, it is usually required by consideration at system level. A coupled control can indeed reduce the overall complexity of the spacecraft. Moreover, in the case of low-thrust solar electric propulsion used for both orbital and attitude control this would probably be the only reasonable solution.

The minimum number of thrusters required to completely control both the orbital and attitude dynamics is twelve, since two thrusters are required for each direction. This redundancy is only required at system level, so six control actions corresponding to the working thrust magnitudes reported below, are considered in the control vector.

$$u = \begin{bmatrix} u_1 \\ u_2 \\ u_3 \\ u_4 \\ u_5 \\ u_6 \end{bmatrix} \Rightarrow \begin{cases} T_X^{+1} = \begin{cases} u_1 & u_1 \geq 0 \\ 0 & u_1 < 0 \end{cases} \\ T_Y^{+1} = \begin{cases} u_2 & u_2 \geq 0 \\ 0 & u_2 < 0 \end{cases} \\ T_Z^{+1} = \begin{cases} u_3 & u_3 \geq 0 \\ 0 & u_3 < 0 \end{cases} \\ T_X^{+2} = \begin{cases} u_4 & u_4 \geq 0 \\ 0 & u_4 < 0 \end{cases} \\ T_Y^{+2} = \begin{cases} u_5 & u_5 \geq 0 \\ 0 & u_5 < 0 \end{cases} \\ T_Z^{+2} = \begin{cases} u_6 & u_6 \geq 0 \\ 0 & u_6 < 0 \end{cases} \end{cases} \begin{cases} T_X^{-1} = \begin{cases} 0 & u_1 \geq 0 \\ -u_1 & u_1 < 0 \end{cases} \\ T_Y^{-1} = \begin{cases} 0 & u_2 \geq 0 \\ -u_2 & u_2 < 0 \end{cases} \\ T_Z^{-1} = \begin{cases} 0 & u_3 \geq 0 \\ -u_3 & u_3 < 0 \end{cases} \\ T_X^{-2} = \begin{cases} 0 & u_4 \geq 0 \\ -u_4 & u_4 < 0 \end{cases} \\ T_Y^{-2} = \begin{cases} 0 & u_5 \geq 0 \\ -u_5 & u_5 < 0 \end{cases} \\ T_Z^{-2} = \begin{cases} 0 & u_6 \geq 0 \\ -u_6 & u_6 < 0 \end{cases} \end{cases} \tag{47}$$

In order to define the thrusters configuration it is necessary to fix the geometry of the spacecraft. In this work a simple box shaped spacecraft with two solar array panels is considered. In figure 3 the thrusters configuration on the spacecraft is reported.

The chosen OACS thrusters configuration allows to decouple the control torques, as each pair of thrusters controls the rotation around a principal axis of inertia. This can be easily seen in the attitude control sub-matrices B_{51} and

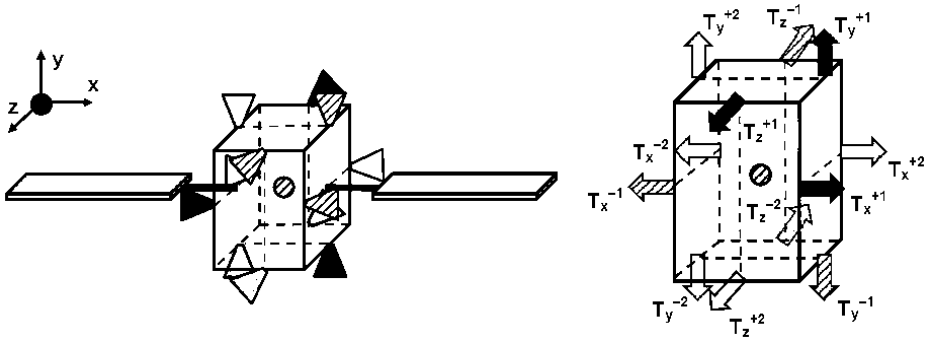

Figure 3: Spacecraft architecture and OACS configuration.

B_{52} where a, b and c represent the three spacecraft dimensions. The orbital control sub-matrices B_{31} and B_{32} depends on the spacecraft orientation, thus realizing the second coupling effect between the two dynamics.

$$B_u(x) = \begin{bmatrix} 0_3 & 0_3 \\ 0_3 & 0_3 \\ B_{31}(x) & B_{32}(x) \\ 0_3 & 0_3 \\ B_{51} & B_{52} \\ 0_3 & 0_3 \\ 0_3 & 0_3 \end{bmatrix} \tag{48}$$

$$B_{31}(x) = B_{32}(x) = \frac{1}{m_d}(\Gamma(x)\Delta)^T \tag{49}$$

$$B_{51} = -B_{52} = {J_d}^{-1}\frac{1}{2}\begin{bmatrix} 0 & 0 & b \\ c & 0 & 0 \\ 0 & a & 0 \end{bmatrix} \tag{50}$$

In order to evaluate the performances of the proposed nonlinear control system it is necessary to identify a detailed model of the thrusters system which allows the identification of saturation levels or other performances degradation factor that should be included in the simulation. Every kind of actuator has its working thrust range and the maximum thrust value is the most important parameter that influences the orbital control performances.

The attitude control action is usually obtained firing thruster in opposite direction to generate a net torque . When both the orbital and attitude control are obtained with the same set of thrusters, the attitude control torque is obtained as a difference in the thrust of the pair of thruster used for translational control. Therefore, the most influencing parameter on the attitude control is the thrust level resolution. This is strictly related to the thrust range (max-min values) and to the actuators electronic driver resolution, typically of 8 bits. All those aspect have been considered in the simulator implementation.

The coupled actuators system has an intrinsic limitation: the attitude control torque cannot be applied correctly if at least one of the thruster necessary is in saturation regime. In order to overcome this limitation, thus guaranteeing a certain level of control torque in each condition, a differential saturation solution has been applied. This solution consists in devoting a minimum thrust interval to the attitude control torque, thus limiting the maximum available thrust for translational dynamics control to a level lower then the physical saturation of the thruster. The amplitude of that interval is computed considering the attitude station-keeping minimal requirements.

Nowadays, different kinds of in-space propulsion thrusters are available.

Low thrust electric propulsion is the best choice for a continuous high-performance application of coupled control. For this reason low-thrust electric propulsion has been chosen and the thrust level has been defined considering the available data for the mission, which indicate the use of eight 40 mN Hall thrusters.

State of the art space sensors can be very accurate for every kind of spacecraft state measure. Therefore, the Kalman-like nonlinear filter proposed in this work is used only for better rejection of the measurement noise.

The SDC system used for the controller design is characterized by a 21-states model which comprises also fictitious stable states used to treat bias terms and integral states. The value of those fictitious stable states is fixed to unity, thus the corresponding terms in the noise weight matrix should be kept sufficiently low. The two integral states of the relative position and MRP are not a physical measure, and so can be neglected by the nonlinear filter. The error on integral states is related to the drift due to the propagation. This drift can be treated erasing the non-physical initial condition at apogee passage, just down-streaming the 15-order Kalman-like nonlinear filter.

4.4. SDRE Timing

Although the computational capability of the recent on board computers would have made possible real and continuous time solution of Riccati equation, it has been decided to implement a timing strategy for the solution of the Riccati equation. In this way the GNC processor computational load can be reduced as the solution of SDRE for both the controller and the nonlinear filter is performed discretely at a certain time step. A linear-like proportional control law is maintained along a time interval with the gain matrix

computed at the beginning of it. This strategy can sensibly reduce the computational load required by the solution of the SDRE in case of high-order SDC systems. Moreover, if the SDC gains are actually slowly varying during the time interval, a continuous solution of the SDRE does not effectively increase the performances of the control system.

The choice of the time step for the SDRE solution of the controller is the next step. Clearly, it is not possible to derive an absolute law for the identification of the SDRE solution time step applied to formation flying. However, a sensitivity analysis has been conducted on formation flying typical scenarios, highlighting some basic guidelines that are applied in this work. Due to HEO characteristics, the evolution of the gains associated with the orbital motion is approximately sinusoidal along the true anomaly. Therefore, assuming a 1% RMS allowable error on gain approximation, it's possible to derive the demanded number of updates per orbit. In the case of Proba-3 orbit, it comes out that 100 updates are sufficient to guarantee the RMS error with respect to the continuous solution. This update frequency is translated into a true anomaly step and then into time step along the orbit using Kepler's equation. The resulting time steps are very fitted during perigee passage, but are more coarse during the central part of the orbit across the apogee.

These time steps would be acceptable if the objective of the controller is related only to station-keeping operation. However, two reconfiguration maneuvers are performed before and after the apogee passage, each one for a duration of 2 hours. During this maneuvering intervals, the SDRE solution time steps previously derived are too coarse to guarantee good performances. For this reason, during the maneuvers the SDRE solution time step is con-

siderably reduced, adding equally spaced time steps. For each maneuver 120 update steps are imposed, neglecting the gain characteristics but verifying that they are sufficient for a 90° relative orbital and attitude maneuver. The SDRE time step for the reconfiguration maneuver is so fixed to 60 s, which provides a maximum angular relative step equal to 1.5°. Figure 4 highlights the resulting time step evolution.

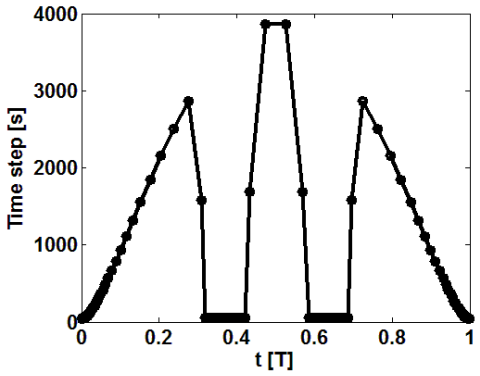

Figure 4: SDRE Timing.

The SDREF solution update time steps choice have been investigated with a corresponding sensitivity analysis. Estimation entails not only application of estimator control law, but also filtering of system dynamics using a numerical integration of the estimated state vector. Moreover, filtering is an action far more sensitive to the time steps duration than the optimal SDRE control, since also the filter matrices A and B should be discretely computed. Due to the HEO characteristics, which have brought to a relatively small time step during the perigee passage, the SDREF update time has been fixed to be the double of the SDRE one, along the entire orbit.

5. Simulation Results

The proposed SDRE coupled control system has been designed and tested considering as scenario the above mentioned Proba-3 mission. The simulations have been carried out using Adams-Bashforth-Moulton numerical propagator, which is a classical Predictor-Corrector variable step method. The choice of the minimum relative tolerance is imposed by the attitude dynamics, since its response time is decisively faster than the orbital one. The numerical propagation is carried out using Cowell's method, in order to maintain the coherence with the state-space algorithm on which the control system is based. Table 1 shows the data used in the numerical simulations for both the chief and deputy satellite. The I.C. column reports the initial condition of the trailing configuration, where ϕ, θ and ψ are the angle representing a 321 Euler angle rotation.

In order to acquire the operative configuration and to go back to the trailing configuration two reconfiguration manoeuvres have been considered with a starting time and angle reported in the following equations:

$$\Delta t = \begin{cases} t - 6.25h \\ t - (13.45h - T_m) \end{cases} \tag{51}$$

$$\theta_{rif} = \begin{cases} -90^\circ \\ 0^\circ \end{cases} \tag{52}$$

where T_m is the single manoeuvre duration and t is the time measured from the perigee passage. The tracking signal for the two orbital reconfiguration

SC	Orbital	I.C.	Attitude	I.C.	Inertial	Prop.
Chief	a (RU)	5.8074	θ (°)	-90	m (kg)	475
	e	0.8062	ϕ (°)	0		
	i (°)	23.439	ψ (°)	0	J_x ($kg\ m^2$)	79
	Ω (°)	0	ω_x (rad/s)	0	J_y ($kg\ m^2$)	272
	ω (°)	160.46	ω_y (rad/s)	0	J_z ($kg\ m^2$)	276
	ν (°)	0	ω_z (rad/s)	0		
Deputy	ρ_r (m)	0	θ (°)	-90	m (kg)	245
	ρ_θ (m)	-150	ϕ (°)	0		
	ρ_h (m)	0	ψ (°)	0	J_x ($kg\ m^2$)	33
	$\dot{\rho}_r$ (m/s)	0	ω_x (rad/s)	0	J_y ($kg\ m^2$)	41
	$\dot{\rho}_\theta$ (m/s)	0	ω_y (rad/s)	0	J_z ($kg\ m^2$)	41
	$\dot{\rho}_h$ (m/s)	0	ω_z (rad/s)	0		

Table 1: Inputs of control system numerical simulations based on Proba-3.

manoeuvres is provided by the following relations:

$$\rho = r \begin{bmatrix} \cos\left(\theta(\Delta t) + \theta_{rif}\right) \\ \sin\left(\theta(\Delta t) + \theta_{rif}\right) \\ 0 \end{bmatrix} \tag{53}$$

$$\dot{\rho} = r\dot{\theta}(\Delta t) \begin{bmatrix} -\sin\left(\theta(\Delta t) + \theta_{rif}\right) \\ \cos\left(\theta(\Delta t) + \theta_{rif}\right) \\ 0 \end{bmatrix} \tag{54}$$

$$\ddot{\theta}(\Delta t) = \pm \begin{cases} \ddot{\theta}_m, \Delta t \leq T_m/2 \\ -\ddot{\theta}_m, \Delta t > T_m/2 \end{cases} \tag{55}$$

$$\dot{\theta}(\Delta t) = \pm \begin{cases} \ddot{\theta}_m \Delta t, \Delta t \leq T_m/2 \\ \dot{\theta}_{m,\max} - \ddot{\theta}_m(\Delta t - T_m/2), \Delta t > T_m/2 \end{cases} \tag{56}$$

$$\theta(\Delta t) = \pm \begin{cases} \frac{1}{2}\ddot{\theta}_m \Delta t^2, \Delta t \leq T_m/2 \\ \frac{1}{2}\ddot{\theta}_m (\frac{T_m}{2})^2 + \dot{\theta}_{m,\max}(\Delta t - T_m/2) - \frac{1}{2}\ddot{\theta}_m(\Delta t - T_m/2)^2, \Delta t > T_m/2 \end{cases} \tag{57}$$

where r is the actual trailing relative distance between the deputy and the chief at the beginning of the manoeuvre and $\dot{\theta}_m$ and $\ddot{\theta}_{m,max}$ are the angular acceleration and the maximum angular velocity of the manoeuvre. Each manoeuvre is divided in two parts with opposite angular acceleration as indicated in Eq. (55-57). Moreover, the orbital angular velocity of Eq. (56) is also used as relative angular velocity to rotate the OS along the out-of-relative-plane direction.

5.1. SDRE Control

The controller design is related to the SDRE update time step and to the control weight matrices. Considering the results of simulations with continuous SDRE solution, the angular step along an orbit has been imposed to 3.6°, resulting in a 1% gain error. The resulting 100 update angular steps are transformed in the corresponding update times along the orbit. In addition, during the two relative manoeuvres, the update time step has been fixed to 60 s.

The weights which compose the weighting matrices have been obtained through a trade-off analysis. The final weight used both in the SDRE and in the SDREF are summarized in table 2. In the SDRE controller design, it has been chosen to fix a common weight Q_{orb} for the nine orbital states and a common weight Q_{att} for the nine attitude states, while R is obviously

unique for the six control actions. Additional state s is not controllable, but stabilizable, so its weight is zero, and the Q matrix is positive-semidefinite.

$$Q_{orb} = 10^5 \qquad Q_{att} = 10^6 \qquad R = 10^{12} \tag{58}$$

5.2. SDREF Estimation

The Kalman-like nonlinear filter design is related to the SDREF update time step choice and to the measurement matrices trade-off. The SDREF update time step has been chosen almost doubling the controller frequency (in fact, with an angular step of 2°), in order to obtain a minimum time step of 25 s during perigee passage, and a time step of 30 s during the manoeuvres.

The measurement matrices weights, presented in table 2, have been chosen with a proper modeling of the sensor static performances. The integral states are neglected by the filter algorithm, while erasing the initial conditions during the apogee passage downstream the filter.

5.3. Control System Performances

The performances of the designed nonlinear coupled control system have been evaluated running simulations based on the Proba-3 scenario outlined above. The obtained results for both the orbital and attitude relative states are reported in figure 5 where the errors on the tracking of the relative position and attitude are shown. In the case of the relative position the error on modulus of the relative distance is reported, while the error on the angle of the Euler axis (as in the Euler axis and angle formalism) is reported for the relative attitude.

The relative position error is maintained below the value of 1 m during both the trailing, the operative and the reconfiguration phases. In particular,

State	SDRE	SDREF
Relative Position Integral	10^5	10^2
Relative Position	10^5	10^{-4}
Relative Velocity	10^5	10^{-4}
Relative MRP	10^6	10^{-10}
Relative Angular Velocity	10^6	10^{-10}
Stable State	0	10^{-6}
Relative MRP Integral	10^6	10^{-6}
Orbital Disturbances	-	10^{-10}
Attitude Control	-	10^{-16}

Table 2: Controller and estimator weights.

error peaks show up during the perigee passage (maximum of the disturbance action level), in the middle of the reconfiguration manoeuvres, where the tracking signal presents a step variation of relative acceleration, and at the apogee passage, due to erasing condition of integral states.

The same considerations can be done observing the relative attitude error, which is maintained under the level of 1°. The performances of the designed Kalman-like nonlinear filter are presented in figure 6 where the error in the reconstruction of the relative distance and on the Euler angle are shown.

The measurement noises have been simulated with reasonable static error performances of the sensors. Both the orbital and the attitude states are reconstructed with adequate rejection of the high frequency noise. The performances of the SDREF are not affected by the reconfiguration manoeuvres; the error in reconstructing the relative position is always one order of magni-

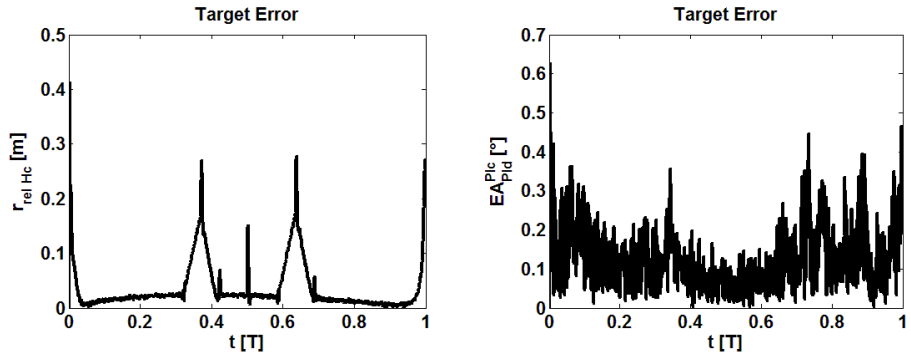

Figure 5: Orbital and attitude control performances.

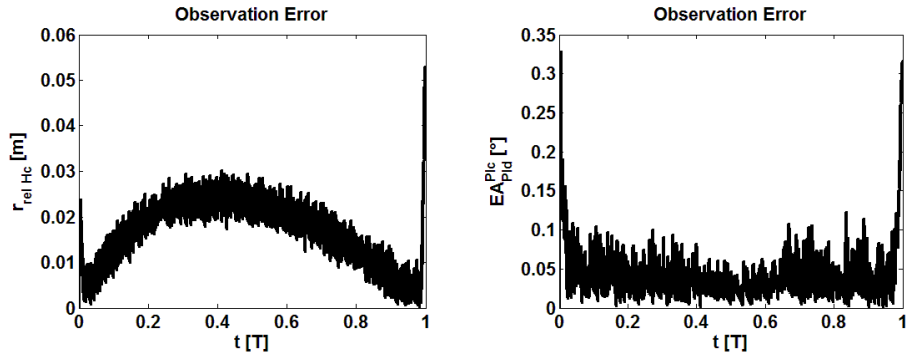

Figure 6: Orbital and attitude states reconstruction.

tude lower than the tracking error, while the reconstructed relative attitude is mostly affected by the perigee passage.

Figure 7 shows the control actions required by the coupled OACS, while figure 8 shows the electrical power required during the entire orbit. The levels of thrust required by the six control actions is compatible with the specification of the Proba-3 thrusters, while the overall electrical power consumption is feasible considering the Proba-3 EPS sizing.

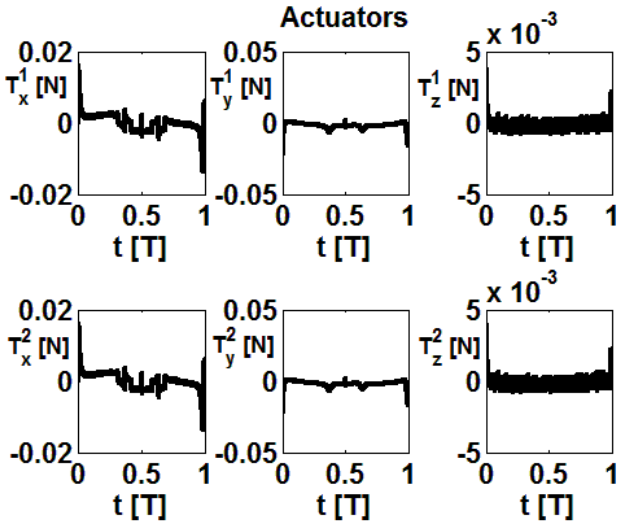

Figure 7: OACS control actions.

6. Conclusion

In this paper, the control of coupled relative position and attitude of a spacecraft in formation flying is solved using the SDRE methodology. The designed control has been tested considering as application scenario the ESA formation mission Proba-3. First of all, a complete dynamical model has been derived for the numerical simulation of the mission scenario. The selected mission is very interesting from the point of view of control system design for Earth formations, since it is specifically designed to qualify and enhance new state-of-the art technologies whcih allow better performances.

The main results that come out from this work are related to the necessity of using a nonlinear model of the dynamics to obtain the high performances and safety levels required by future formation mission. Those formations will require very close coordinated relative manoeuvres on non-circular orbits,

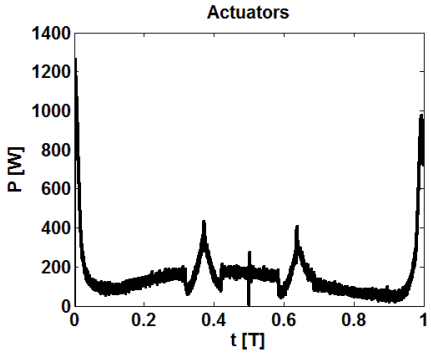

Figure 8: OACS electrical power consumption.

thus requiring very accurate control but retaining the need of the reduction of fuel consumption. Therefore, the SDRE methodology is perfect as it allows to apply systematically the optimal control theory to a nonlinear model which is more representative of the dynamics. Moreover, the use of a timed update strategy for the solution of the State-Dependent Riccati Equation has been proved to be feasible in the limit case of HEO, thus reducing the computational requirement associated. Finally, the results obtained with the designed coupled control system prove that the SDRE technique can be effective even in the case of completely coupled orbital and attitude relative manoeuvres, allowing the simplification of the spacecraft design at system level.

References

[1] D. C. Redding, N. J. Adams, E. T. Kubiak, Linear-quadratic station-keeping for the sts orbiter, Journal of Guidance, Control, and Dynamics 12 (1989) 248–255.

[2] V. Kapila, A. G. Sparks, J. M. Buffington, Q. Yan, Spacecraft formation flying: Dynamics and control, Journal of Guidance, Control, and Dynamics 23 (3) (2000) 561–564.

[3] K. Alfriend, H. Schaub, Dynamics and control of spacecraft formations-challenges and some solutions, in: The Richard H. Battin Astrodynamics Symposium, College Station, TX, 2000, pp. 205–223.

[4] D. Gim, K. Alfriend, The state transition matrix of relative motion for the perturbed non-circular reference orbit, in: Proceedings of the 11 th Annual AAS/AIAA Space Flight Mechanics Meeting, Santa Barbara, CA, 2001, pp. 913–934.

[5] K. Alfriend, H. Schaub, D. Gim, Gravitational perturbations, nonlinearity and circular orbit assumption effects on formation flying control strategies, in: 23rd Annual AAS Guidance and Control Conference, 2000, pp. 2–6.

[6] P. Wang, F. Hadaegh, Coordination and control of multiple microspacecraft moving in formation, Journal of the Astronautical Sciences 44 (3) (1996) 315–355.

[7] H. Pan, V. Kapila, Adaptive nonlinear control for spacecraft formation flying with coupled translational and attitude dynamics, in: Decision and Control, 2001. Proceedings of the 40th IEEE Conference on, Vol. 3, IEEE, 2001, pp. 2057–2062.

[8] B. Naasz, M. Berry, H. Kim, C. Hall, Integrated orbit and attitude

control for a nanosatellite with power constraints, Advances in the Astronautical Sciences 114 (2003) 9–25.

[9] J. Slotine, W. Li, Applied nonlinear control, Prentice-Hall, Englewood Cliffs, NJ, 1991.

[10] M. Krstic, P. Kokotovic, I. Kanellakopoulos, Nonlinear and Adaptive Control Design, John Wiley & Sons, Inc., 1995.

[11] J. R. Cloutier, C. N. D'Souza, C. P. Mracek, Nonlinear regulation and nonlinear H_∞ control via the state-dependent riccati equation technique; part 1: Theory, in: Proceedings of the First International Conference on Nonlinear Problems in Aviation and Aerospace, Daytona Beach, Florida, 1996.

[12] J. R. Cloutier, C. N. D'Souza, C. P. Mracek, Nonlinear regulation and nonlinear H_∞ control via the state-dependent riccati equation technique; part 2: Examples, in: Proceedings of the First International Conference on Nonlinear Problems in Aviation and Aerospace, Daytona Beach, Florida, 1996.

[13] J. Cloutier, D. Stansbery, The capabilities and art of state-dependent riccati equation-based design, in: American Control Conference, 2002. Proceedings of the 2002, Vol. 1, IEEE, 2002, pp. 86–91.

[14] K. Hammett, C. Hall, D. Ridgely, Controllability issues in nonlinear state-dependent riccati equation control, Journal of Guidance Control and Dynamics 21 (5) (1998) 767–773.

[15] J. Cloutier, D. Stansbery, Nonlinear, hybrid bank-to-turn/skid-to-turn missile autopilot design, in: AIAA Guidance, Navigation, and Control Conference and Exhibit, Montreal, Canada, 2001.

[16] D. Stansbery, J. Cloutier, Position and attitude control of a spacecraft using the state-dependent riccati equation technique, in: American Control Conference, 2000. Proceedings of the 2000, Vol. 3, IEEE, 2000, pp. 1867–1871.

[17] C. Mracek, J. R. Cloutier, C. D'Souza, A new technique for nonlinear estimation, in: Control Applications, 1996., Proceedings of the 1996 IEEE International Conference on, IEEE, 1996, pp. 338–343.

[18] X. Leyre, Proba-3, formation flying demonstration mission. phase a summary report. esa contract 20015/06/nl/ja for thales alenia space., Tech. rep., ESA (2007).

[19] S. Marandi, V. Modi, A preferred coordinate system and the associated orientation representation in attitude dynamics, Acta Astronautica 15 (11) (1987) 833–843.

[20] T. Çimen, State-dependent riccati equation (sdre) control: A survey, in: World Congress, Vol. 17, 2008, pp. 3761–3775.